

## DATA EXTRACTION FROM CARTE DU CIEL TRIPLE IMAGES

Lasko M. Laskov, Milcho Tsvetkov

ABSTRACT. *Carte du Ciel* (from French, *map of the sky*) is a part of a 19th century extensive international astronomical project whose goal was to map the entire visible sky. The results of this vast effort were collected in the form of astrographic plates and their paper representatives that are called *astrographic maps* and are widely distributed among many observatories and astronomical institutes over the world. Our goal is to design methods and algorithms to automatically extract data from digitized Carte du Ciel astrographic maps. This paper examines the image processing and pattern recognition techniques that can be adopted for automatic extraction of astronomical data from stars' triple expositions that can aid variable stars detection in Carte du Ciel maps.

**1. Introduction.** Carte du Ciel, together with the Astrographic Catalogue, formed a vast international project that started in 1887 [9] and continued until 1962 [4]. The ambitious goal of this project was to create a catalogue of

---

*ACM Computing Classification System* (1998): I.4, I.4.6, I.4.8, J.2.

*Key words:* Astrographic maps, Carte du Ciel, scientific heritage, image processing, pattern recognition.

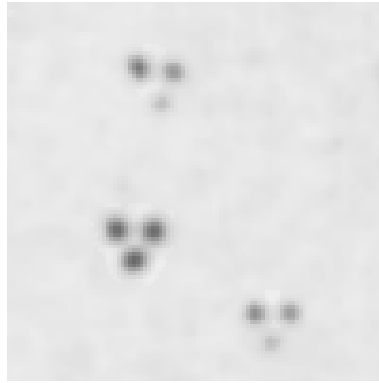


Fig. 1. A fragment of scanned Carte du Ciel astrographic map. Three triples of stars images (asterisms) are visible, each corresponding to a singles star

the positions of the stars in the visible sky as faint as 11th magnitude<sup>1</sup> and to represent the relative positions of the stars of 14th magnitude and brighter [14]. The idea was to incorporate the new (at that time) technology of photography in the process of creation of the atlas of the sky, and around 20 observatories worldwide agreed to participate in the project.

Carte du Ciel itself was the more ambitious part of the project since its aim was to map the entire sky down to 14th magnitude. Each photographed field would be with dimensions  $2^\circ \times 2^\circ$ , and the corner of each plate would be at the center of its neighbour [4]. Unfortunately this goal turned to be too expensive both as effort and technology that was required at the time, and some of the observatories did not even start this part of the project and completed only the Astrographic Catalogue. However, some of the participants did the tasks required for the Carte du Ciel, and the resulting photographic plates still exist, providing extremely important data for astronomers mainly because of their age: many of the plates are nearly 100 years old.

The approach that was used to produce the Cart du Ciel charts was to use photographic plates with dimensions  $12\text{ cm} \times 12\text{ cm}$  with triple exposure for about 20 minutes each. The reproduction of the charts into astrographic maps was using the technique of the photogravure on copper plates that were used to produce the paper copies. Because of the triple exposure, each star is represented by three images on the plate (see Fig. 1) that form the vertices of an equilateral triangle. The reason why three exposures on the same plate were made was to be

---

<sup>1</sup>Magnitude or photographic magnitude  $m$  is a logarithmic measure of a celestial object's brightness  $I$ . The lower magnitude, the brighter the object is ( $m = -2.5 \log_{10}(I)$ ).

able to distinguish stars' images from plate failures and defects, and from other celestial bodies such as asteroids, for example.

The three images of each star that are result of the triple exposure, or *asterism*, as they are called by Fresneau [2], were used to calculate the exact position of the star. On the other hand, these images can contain valuable information about the star being observed – a significant difference between the three images in an asterism could indicate an astronomical event such as stellar explosion that occurred during the plate exposures or could indicate that the star is a close binary system variable. It is important to note that if such an event is detected, it will bring important information to specialists in the field because of the epoch the event is actually photographed on the plate.

Even though the common approach is to examine manually the Carte du Ciel data, this task is quite expensive and time consuming mainly because of the size and resolution of the images, and the number of asterisms that are contained, as well. A number of image processing and pattern recognition techniques can be adopted to assist this research or even to fully automate astronomical events detection in the plates, both saving time and cost, and enhancing the productivity and accuracy of the process.

The goal of this paper is to produce a preliminary survey and analysis of the image processing and pattern recognition techniques that will be adopted in the design of a software tool for celestial event detection that are captured in the Carte du Ciel maps. The main task performed by this software will be to detect each asterism that is contained in a given map, and to automatically analyse the three images for significant difference between the standard deviations  $\sigma$  of each of the Gaussian that model the constituting stars.

This paper is organized as follows. In the next section called *Related work*, three papers that are used as a starting point for our research are briefly described. In the section *Carte du Ciel triple image characteristics* the features of the input images are investigated. These considerations give the background for the image processing techniques that are discussed in the subsequent sections. In the fourth section, *Segmentation*, some methods for image segmentation that are applicable in the case of the examined images are described. The fifth section, *Asterism detection*, discusses the algorithms that can be adopted for triple star image extraction from the digitized plates.

**2. Related work.** In [14] the problem of reduction of the Astrographic Catalogue plates is investigated. Even though the input data are the plates that are a result of the Astrographic Catalogue part of the project, there are many

considerations that are also important in the case of digital processing of Carte du Ciel astrographic maps. The plate model that is investigated by the author is consisted of four orthogonal terms ( $a, b, c, d$ ), two non-orthogonal terms ( $e, f$ ), and two tilt terms ( $p, q$ ):

$$(1) \quad \xi = ax + by + c + ex + fy + x^2p + xyq$$

$$(2) \quad \eta = ay - bx + d - ey + fx + xyp + y^2q$$

where  $x$  and  $y$  denote the coordinates measured on the plate, and  $\xi$  and  $\eta$  are the standard coordinates (see also [12] and [13]).

The following distortions have been considered in further model modification: radial distortion, tangential distortion, magnitude equation, coma<sup>2</sup>, periodic measuring errors, etc. The author stresses that the development of the plate models will become trivial if the systematic errors in the plates are discovered and corrected. These correction methods should consider mismatched stars images, blended images of multiple stars, and typographical errors.

In the work [10] the authors describe a method for reduction of astrographic plates that have been produced in the Carte du Ciel project. The approach is based on modelling each individual asterism (triple exposure of each star) using the sum of three bivariate Gaussian distributions. Two models are examined. The first one is based on 22 free parameters, and the density for each pixel ( $i, j$ ) is calculated:

$$(3) \quad D_{ij} = B \sum_{k=1}^3 A_k \exp \left\{ -\frac{1}{2} \left[ \frac{1}{1-t_k^2} (X^2 + Y^2 - 2t_kXY) \right]^{s_k} \right\},$$

where

$$(4) \quad X = \frac{x_{ij} - x_{ck}}{\sigma_{xk}}, Y = \frac{y_{ij} - y_{ck}}{\sigma_{yk}},$$

and  $B$  is the background of the frame containing the asterism,  $A_k$  is the peak density of the  $k$  th frame,  $x_{ij}$ ,  $y_{ij}$  are the pixel coordinates, and  $\sigma_{xk}$ ,  $\sigma_{yk}$ ,  $t_k$  are the parameters of an ellipse.  $s_k$  is a parameter that is used to describe the saturation of the photographic emulsion.

A non-linear square fitting procedure is implemented based on the Levenberg-Marquardt method [8] that is applied to the above model. Also, the authors propose a reduction of (3) to a model with 12 free parameters, assuming that the

---

<sup>2</sup>Comatic aberration is an optical aberration that is a result of optical design or lens imperfection which can result in stars appearing to have comet-like tails.

three exposures should be identical. The later makes the application of this scheme for our task not directly applicable. On the other hand, many of the possible plate distortions are examined in [10], such as presence of perpendicular grid in the images, Kostinsky effect<sup>3</sup> [5], optical aberrations such as coma, spherical aberrations, field curvature and chromatic distortions.

Even though presumably connected, the above-mentioned works do not specifically investigate the problem of celestial event detection in the Carte du Ciel plates. Actually, there are very few attempts in the literature to exploit the potential of the data contained in these images to detect changes in the stars' magnitude that occurred during the triple exposure of the plates.

Such a work is the one described in [2] in which the authors describe an approach for variable star detection in the Carte du Ciel plates, using the fact that the images contain triple exposures of the concrete part of the sky. The procedure that is used to segment triple exposures of each star is the same that is used by [10] (see also (3)) to separate the stellar images from plate imperfections. The result of the segmentation step is a catalog of all detected stars with their coordinates and magnitudes taken as the mean value of the respective three images with their mean square deviation. The stars that have mean square deviation larger than 0.4 are considered as variable star candidates. The authors do not investigate the case when one of the star images is missing in a given asterism.

Unfortunately the authors do not give a detailed information about the image processing techniques and algorithms that are used in the presented research.

In this paper we will focus exactly on these algorithms that can significantly speed up and improve the processing of Carte du Ciel astrographic maps, especially in the case of variable stars detection in order to register celestial events a century-old.

**3. Carte du Ciel triple image characteristics.** Our data set is composed of Carte du Ciel images of digitized astrographic maps that have been taken in the Brussels zone ( $+32^\circ$ ,  $+39^\circ$ ) at the Royal Observatory of Belgium. We dispose with the paper copies (maps) of the astrographic plates that have been produced using the technique of photogravure on copper plates. It is important to note that the maps themselves represent a magnified version of the astrographic data since their scale compared with the plates is 2 : 1.

---

<sup>3</sup>In photography, a development effect in which two close dark image regions appear to move apart, while two close light image regions appear to move closer together.

The scanning of the astrographic paper copies is performed using a Zeutschel Overhead Scanning System OS 12000 Advanced. The images are scanned in gray scale with 8 bits per pixel, with resolution of 600 ppi. For the purposes of our research this resolution is more than sufficient because it corresponds approximately to 40 mic/mm on the paper surface, and a higher resolution would result in a redundant texture captured in the output bitmap. The resulting images are relatively big in dimensions:  $8750 \times 8926$  pixels.

The image structure can be separated into two general parts: (i) the main part of the image in the image center that contains the copy of the astrographic plate with stellar images; (ii) image border that contains plate meta-data (coordinates of the center of the plate, plate number, the observatory in which the instrument is located, the date and the exact sidereal time when the exposures were taken, duration of exposure, the name of the observer), and correspondence between stellar images masses and apparent magnitude of the stars (see Fig. 2).

Even though in this study we will focus mainly on processing the central part of the image, some of the data in the image border can be extremely useful, for example the magnitude chart mentioned above (Fig. 2) can be used to label automatically the segmented stellar images with their corresponding apparent instrumental magnitudes.

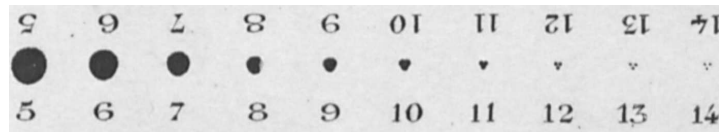


Fig. 2. Fragment of the border region of a scanned plate that contains the correspondence between the masses of the stellar images and stars apparent magnitude

An important feature of the map images is the presence of a perpendicular grid. Each map contains 25 horizontal and 25 vertical straight lines that partition it into 676 square regions or sub-images. This grid forms a coordinate system with its beginning placed in the geometrical center of the plate. Each horizontal and vertical line of the grid is numbered starting from 0 from the center and increasing the respective number in both directions (left-right for horizontal and up-down for vertical) with a step equal to 5. Thus the lines have the following numbers associated to them:  $60, \dots, 10, 5, 0, 5, 10, \dots, 60$  for both horizontal and vertical case (see also Fig. 3).

The grid in the Carte du Ciel plates certainly is a useful tool for the specialists who measure manually these images, but unfortunately the lines overlap many asterisms thus making the information about the respective stars generally

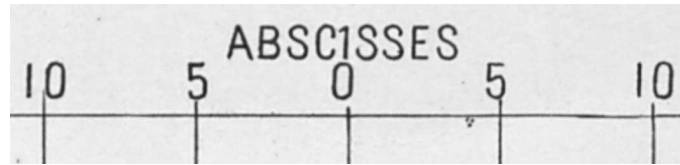


Fig. 3. The fragment from the central part of the vertical lines' numbering. The same numbering is used for the horizontal lines of the grid

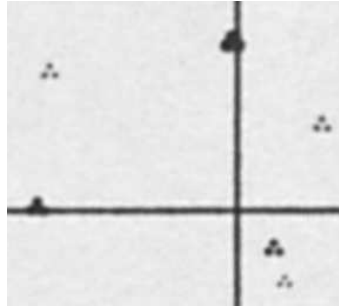


Fig. 4. Both the horizontal and the vertical line of the grid are overlapping an asterism thus making useless the information about these two stars

useless or even lost (see Fig. 4).

In the above context it has to be noted that the width of a grid line in pixels is approximately 12, which is enough as size to cross out completely an asterism with an approximate width of 23 pixels, such as the asterisms of 14th magnitude. What is more, it is enough for a single star to be overlapped to confuse the methods and procedures for variable stars detection. Based on these considerations, in our research we will ignore the asterisms that are overlapped by the grid lines. In other words, the area of the images that is going to be processed is the one contained in the 676 sub-images formed by the grid, without the grid itself. Since the image illumination is uniform and the sub-images' characteristics are similar, we can process each of the sub-images individually using the same procedures.

The advantage of the separate processing of the plate sub-images is that the intermediate results for a plate can be observed. Processing the whole plate at once can be a time-consuming operation, because of the image size in pixels and the relatively small mass of the minimal wrapping windows of the asterisms that has to be detected and analyzed.

Another major difficulty in Carte du Ciel plate image processing can be observed when the exposures of two or more stars are projected too close on



Fig. 5. An example of overlapping asterisms. Five stars' exposures are too close on the plate, which results in their merging

the plate. This can cause asterisms to merge, as shown in Fig. 5. In the case of overlapping asterisms special methods for segmentation have to be applied. Unfortunately, such kind of overlapping can cause the data for a star to be too hard to be extracted, or even to be lost.

**4. Noise reduction and segmentation.** Most of the image processing and pattern recognition in image procedures starts with preliminary processing routines for image quality enhancement and noise reduction. These routines may significantly speed up the whole process by enhancing the subsequent algorithms, but on the other hand they must be applied with care, because apart from noise reduction they can result also in important data loss.

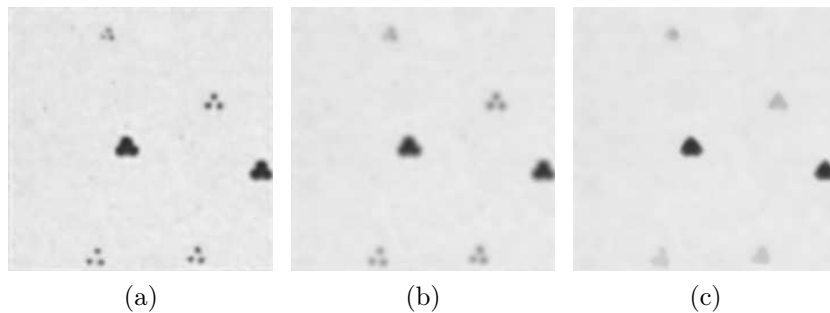


Fig. 6. The original fragment (a) filtered with: (b) Gaussian filter with size 9 and variance  $\sigma = 2$ ; (c) median filter with size 9

In the case of Carte du Ciel images processing noise reduction filters, such as Gaussian filters and median filters (see [3]), will have generally two effects. The



first effect which we can consider as positive, is the background smoothing which results in less noise regions that can be incorrectly detected as star images in the subsequent steps. The second effect is obviously negative: blurring of the star images (see Fig. 6(b) for Gaussian filtering and Fig. 6(c) for median filtering). The star image blurring causes changes in stars variances and asterisms merging into a single blob that can impede variable stars' detection and even asterism segmentation.

Indeed, a closer look at Fig. 6 shows that both Gaussian and median filters significantly reduce the noise in the original image Fig. 6(a), but both filters cause star image blurring and merging of the asterisms. From these observations we can conclude that noise reduction and image smoothing can be used as a preliminary step before background segmentation, but variable star detection algorithms must work with the original asterisms extracted from the original input image, which is achievable since smoothing is not going to change the location of the stars images in pixel coordinates.

After the preliminary noise reduction, the next step in plate image processing is to separate the pixels that belong to objects from the pixels that belong to the background. Since background pixels are usually labeled with white color or gray-scale value 255, and object pixels are labeled with black color or gray-scale value 0, this process is often referred as *binarization*. The other term that is usually used in the literature is *background segmentation*.

There are two major issues that have to be addressed when choosing an appropriate binarization algorithm: (i) the homogeneity of the illumination over the entire input image; (ii) the separability of the two classes – background and object pixels.

Since the investigated images are acquired using specialized hardware (the scanner mentioned in Section 2), the image illumination on the entire image domain is homogeneous. What is more, if we analyse the histograms of randomly selected sub-images from different regions of a plate, we will observe that their shapes and gray-levels distributions are nearly identical (see Fig. 7), which unambiguously proves the above assumption.

To evaluate the separability of the background and object pixel classes, we adopt Otsu's discriminant criterion measure  $\eta$ , which is described in detail in [11]:

$$(5) \quad \eta = \frac{\sigma_B^2(k)}{\sigma_T^2},$$

where  $\sigma_B^2(k)$  denotes the intraclass variance,  $\sigma_T^2$  denotes the total variance for the whole histogram, and  $k$  denotes the threshold that separates the values that

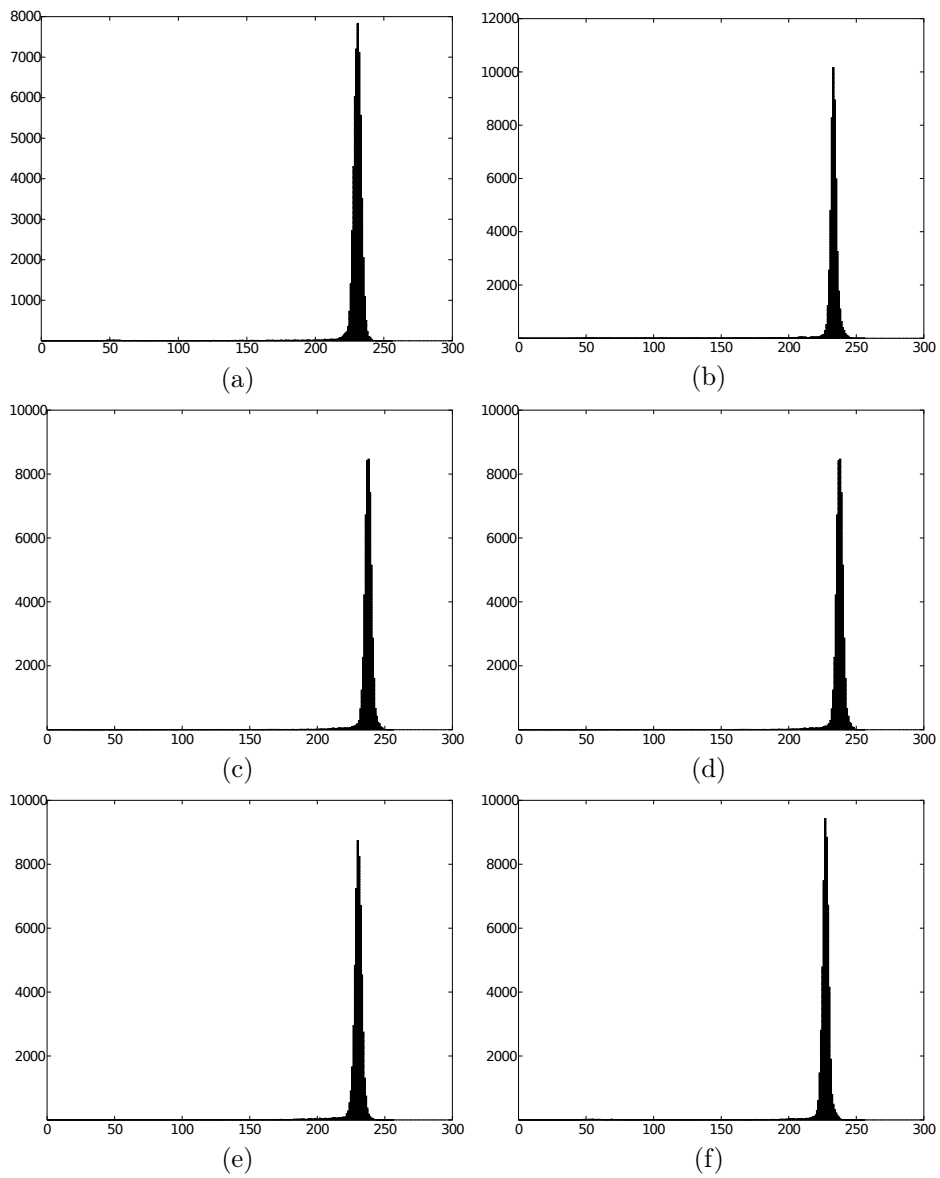


Fig. 7. Gray-level histograms of six randomly selected sub-images of the input plate. The shapes and gray-level distributions show homogeneous illumination of the plate

are labeled as object pixels (black pixels)  $[0, k]$  and values that are labeled as background pixels (white pixels)  $(k, 255]$ . An optimal threshold  $k^*$  is selected by maximizing the intraclass variance, because the total variance  $\sigma_T^2$  does not depend on the threshold  $k$ :

$$(6) \quad \sigma_B^2(k^*) = \max_{1 \leq k < 255} \sigma_B^2(k).$$

Then the optimal separability measure  $\eta^*$  is defined as  $\eta^* = \eta(k^*)$ . From this definition it can be easily shown that  $0 \leq \eta^* \leq 1$ , and  $\eta^* = 0$  for images that contain only a single gray-scale value, while  $\eta^* = 1$  when the input image is binary (composed only by black and white pixels).

Using Otsu's separability measure given in equation (5) we obtain the following results for the histograms in Fig. 7 of the six randomly selected sub-images in the original plate, which are given in Table 1. The values of  $\eta^*$  that are obtained for the sub-images are above 0.7 which suggests that the histograms are bi-modal, or in other words, the two classes of background and object pixels are well distinguished in the histograms.

Table 1. The separability measure  $\eta^*$  and the optimal threshold  $k^*$  for the histograms in Fig. 7 calculated by Otsu's method

<b>Histogram</b>	$\eta^*$	$k^*$
Fig. 7(a)	0.806205	166
Fig. 7(b)	0.834544	169
Fig. 7(c)	0.762253	185
Fig. 7(d)	0.762253	185
Fig. 7(e)	0.740119	179
Fig. 7(f)	0.859654	159

Also, the difference between the  $\eta^*$  for the different sub-images is strictly less than 0.15, and the difference between the optimal thresholds is strictly less than 25 in terms of gray-scale values. This means that we can apply Otsu's global method for image binarization on the entire plate domain, and no local binarization method is necessary for the examined images.

If we go back to the fragment in Fig. 4 that contains also a horizontal and a vertical lines of the plate's grid, we will observe that Otsu's method correctly discovers the grid lines pixels together with the pixels that belong to asterisms (see Fig. 8). In other words, Otsu's method can be successfully used as a preprocessing step for the subsequent stage of grid line segmentation.

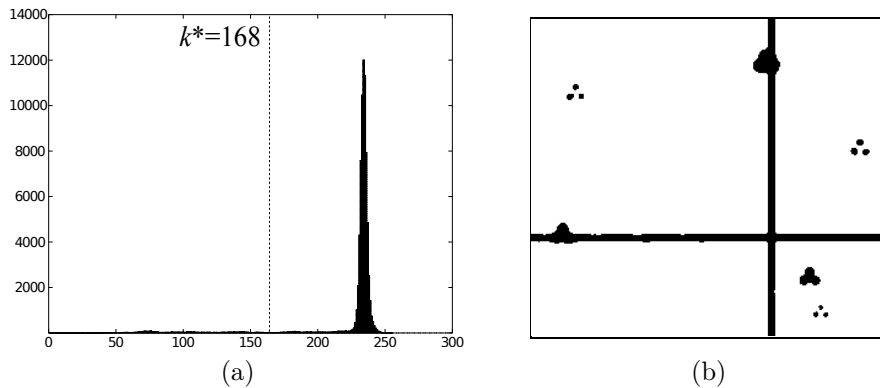


Fig. 8. The gray-level histogram (a) of the fragment in Fig. 4 with the optimal threshold  $k^* = 168$  calculated by Otsu's method, and the resulting binary image (b)

The next key stage in Carte du Ciel plates image processing is the grid detection, since the location of the grid lines will be used to divide the input plate into 676 sub-images. Also, the star images that are intersected by the grid lines will be ignored to avoid false variable star detection. Two completely different approaches are examined here. The first one is based on the Hough transform [1] for straight line detection, and the second one is based on wavelet decomposition of the horizontal and vertical projective profiles of the binary image of the plate [6].

The Hough transform [1] is a standard method in image processing to detect geometrical features even in relatively noisy images. In its form to detect straight lines, a line is represented with its equation in normal form:

$$(7) \quad x \cos \theta + y \sin \theta = \rho,$$

where  $\rho$  is the distance between the origin of the coordinate system and the line, and  $\theta$  is the angle between the normal from the line and the  $x$ -axis. For any point  $(x, y)$  that lies on the line  $\rho$  and  $\theta$  have the same values. The algorithm is based on a voting scheme in which each pixel that belongs to an edge in the input image is mapped to a discrete sinusoid in the  $(\rho, \theta)$  Hough parameter space. The points in which sinusoids intersect determine the straight lines in the input image (see Fig. 9).

The second approach for grid line segmentation is based on the discrete wavelet decomposition of the projective profile of the binary image  $I_{M \times N}(x, y)$

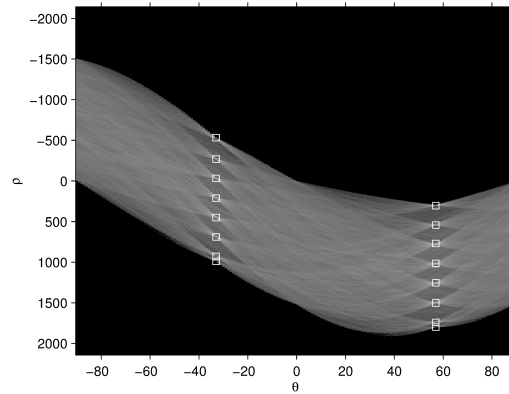


Fig. 9. Hough parameter space of a plate fragment. The white squares indicate the intersection points of the discrete sinusoids that are recognized as straight lines in the original image

[6]. The horizontal profile of  $I$  is defined as

$$(8) \quad h(y) = \sum_{i=0}^{N-1} I(i, y), \quad y = 0, 1, \dots, M-1.$$

The vertical projective profile of  $I$  is defined analogously to (8). Then the method is based on calculation of the approximation part  $A_{2^j}^d h$  of the wavelet decomposition of the profile  $h$  at a given resolution  $2^j$ , and extraction of the local extrema which correspond to the grid lines in the input image. The approximation part of the profile is given by the convolution (for more details see [7]):

$$(9) \quad A_{2^j}^d h = \{(h(u) \circ \phi_{2^j}(-u)) (2^{-j}n)\}_{n \in \mathbf{Z}}.$$

**5. Asterism detection.** Once a plate image is successfully segmented in the previous processing steps, the next efforts will be towards asterism detection and processing. Again, the Hough transform can be adopted for this purpose, but this time in its version for circle detection, to locate the stars images in the plate.

The Circular Hough Transform (CHT) is based on the circle equation:

$$(10) \quad (x - a)^2 + (y - b)^2 = r^2,$$

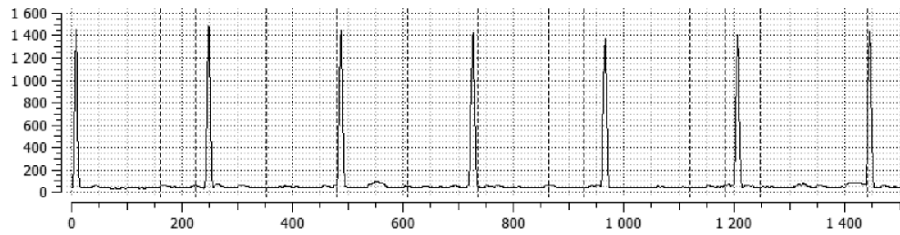


Fig. 10. Horizontal projective profile of a plate fragment with local minima and maxima discovered in the approximation part of the wavelet decomposition of the signal

where  $(a, b)$  are the coordinates of the circle center, and  $r$  is the radius. In parametric form the circle is represented by:

$$(11) \quad \begin{aligned} x &= a + r \cos \theta \\ y &= b + r \sin \theta \end{aligned}$$

The equations (11) are used to build the Hough accumulation space of three dimensions  $(a, b, \theta)$ .



Fig. 11. Circles detected by a CHT algorithm in the plate fragment given in Fig. 4

The voting scheme that is used in the CHT is analogous to the one in the standard Hough transform, described in the previous section. The local maxima in the three-dimensional accumulation space  $(a, b, \theta)$  correspond to the detected circular objects in the input image (see Fig. 11). However, in our case an additional procedure must be defined to discard the “false” circles detected by CHT. Such a procedure can be easily implemented based on the local pixel statistics in the detected circles and the background segmentation threshold calculated by Otsu’s method in the background segmentation step.

**6. Conclusion.** A major purpose of the presented research is to stimulate the analysis of the Carte du Ciel archive observations that are part of the database `wppdb.org` and are included in the catalogue of archives `CWFPA v.6.1`. A small part of the existing Carte du Ciel maps are digitized and are accessible as data for research within the virtual observatory.

In this paper an overview is given of some of the key image processing and pattern recognition methods that are applicable in data extraction from Carte du Ciel maps. The preliminary set of experiments was conducted and the results were presented here to verify that the examined methods can give a good background for development of an integrated software tool which will assist astrophysicists in the investigation of century-old astrographic data. The most ambitious goal of such software is the automatic detection of variable stars that were captured on the astrographic plates. In order to achieve it the following basic steps must be provided by the examined methods: (i) noise reduction and image enhancement without asterism blurring; (ii) image segmentation, grid detection and intersected star images detection; (iii) asterism detection and analysis. Also, some additional processing of the image border may be provided to extract meta-data information for the corresponding plate and data such as the correspondence between the asterisms' mass and stars' apparent magnitude (see Fig. 2).

**Acknowledgements.** We acknowledge the grant of Bulgarian National Science Found – BG NSF DO-02-273/275 and thank Viktoria Naumova for the help in digitalization of the paper copies of the Brussels Carte du Ciel zone and especially Thierry Pauwels for providing the Carte du Ciel copies.

#### REFERENCES

- [1] DUDA R. O., P. E. HART. Use of the Hough Transformation to Detect Lines and Curves in Pictures. *Comm. ACM*, **15** ( 1972), 11–15.
- [2] FRESNEAU A., R. W. ARGYLE, G. MARINO, S. MESSINA. Potential of Astrographic Plates for Stellar Flare Detection. *The Astronomical Journal*, **121** (2001), 517–524.
- [3] GONZALEZ R. C., R. E. WOODS. Digital Image Processing, 3 edition, Prentice Hall, 2007.
- [4] JONES D. The Scientific Value of the Carte du Ciel, *Astronomy & Geophysics*, **41** (2000), No 5, 5.16–5.21.
- [5] Kostinsky, S., Mitt. Nikolai-Hauptsternwarte, Pulkovo, Band II, 14, 1907.

- [6] LASKOV L. Application of Wavelet Decomposition to Document Line Segmentation. *Serdica J. Computing*, **6** (2012), No 2, 149–162.
- [7] MALLAT S. A theory for multiresolution signal decomposition: the wavelet representation. *IEEE Transactions on Pattern Analysis and Machine Intelligence*, **11** (1989), 674–693.
- [8] MARQUARDT D. W. An Algorithm for Least-Squares Estimation of Nonlinear Parameters. *Journal of the Society for Industrial and Applied Mathematics*, **11** (1963), No 2, 431–441.
- [9] MOUCHEZ E. La photographie astronomique a l’Observatoire de Paris et la carte du ciel. Gauthier-Villars, Paris, France, 1887.
- [10] ORTIZ-GIL A., M. HIESGEN, P. BROSCHE. A New Approach to the Reduction of “Carte du Ciel” plates. *Astronomy and Astrophysics Suppl. Ser.*, **128** (1998), No 3, 621–630.
- [11] OTSU N. A threshold selection method from gray-level histograms. *IEEE Transactions on Systems, Man and Cybernetics*, **9** (1979), No 1, 62–66.
- [12] URBAN S. E., J. C. MARTIN, E. S. JACKSON, T. E. CORBIN. New Reductions of the Astrographic Catalogue: Plate Adjustments of the Algiers, Oxford 1, Oxford 2, and Vatican zones. *Astronomy and Astrophysics Suppl. Series*, **118** (1996), 163–167.
- [13] URBAN S. E., T. E. CORBIN. New Reductions of the Astrographic Catalogue: Conventional Plate Adjustment of of the Cape Zone. *Astronomy and Astrophysics*, **305** (1996), 989–998.
- [14] URBAN S. E. Reductions of the Astrographic Catalogue. Dynamics and Astrometry of Natural and Artificial Celestial Bodies, Kluwer Academic Publishers, 1997, 493–498.

Lasko Laskov  
New Bulgarian University  
Informatics Department  
21, Montevideo Str.  
1618, Sofia, Bulgaria  
e-mail: llaskov@nbu.bg

Milcho Tsvetkov  
Institute of Mathematics and Informatics  
Bulgarian Academy of Sciences  
Acad. G. Bonchev Str., Bl. 8  
1113 Sofia, Bulgaria  
e-mail: milcho.tsvetkov@gmail.com

Received February 4, 2014

Final Accepted June 5, 2014